Nonlinear instability of a thin film flowing down a smoothly deformed surface

L. A. Dávalos-Orozco
Instituto de Investigaciones en Materiales, Departamento de Polímeros, Universidad Nacional Autónoma de México, Ciudad Universitaria, Circuito Exterior S/N, Delegación Coyoacán, 04510 México D. F., Mexico

(Received 21 September 2006; accepted 29 May 2007; published online 13 July 2007)

Here, the nonlinear flow instability of a thin film flowing down an inclined wall with smooth deformations is investigated. A nonlinear evolution equation is obtained under the small wavenumber approximation. This equation describes the film free surface deformation including the effects of inertia, viscosity, surface tension, and deformation of the wall. The equation has a forcing term that corresponds to periodic time-dependent perturbations hitting on the free surface. These time-dependent perturbations are tested against the presence of the free surface waves due to wall deformations. In particular, a wall sinusoidal profile is investigated. It is found that when the wall wavelength is small enough, the valleys of the surface response to the wall profile become very deep, showing a kind of resonance, which has an important stabilizing influence in the evolution of the superposed time-dependent perturbations. © *2007 American Institute of Physics*.
[DOI: 10.1063/1.2750384]

I. INTRODUCTION

Research on thin liquid films flowing down walls has been the subject of many papers in the past 40 years due to the important applications this area has on the coating and cooling of walls. Reviews of coating processes can be found in Weinstein and Ruschak[1] for flat and curved surfaces and Quéré[2] for fiber coating. From the theoretical point of view, Yih[3] investigated the linear instability of the liquid films. Lin[4] calculated criticality curves for the Tollmien-Schlichting waves and surface waves corresponding, respectively, to a large and small magnitude of the product of the wavenumber times the Reynolds number. Floryan *et al.*[5] investigated the instability for small angles of inclination of the wall, and in particular they concentrated on the shear modes. Nonlinear surface waves on thin films have been investigated by Benney,[6] who obtained a nonlinear evolution equation, the Benney equation, in the small wavenumber approximation. A normal mode analysis of this equation was done by Gjevik.[7] The growth rate and the curves of criticality can be obtained from the linearized version of the Benney equation. However, Gjevik[7] obtained the subcriticality curve, below which it is supposed that the nonlinear waves do not saturate. An extension to three dimensions of the Benney equation was calculated by Roskes.[8] In the very strong surface tension approximation, Sivashinsky and Michelson[9] demonstrated that this equation reduces to the Kuramoto-Sivashinsky equation, which has been shown to present chaotic behavior. Different approximations to the nonlinear surface wave on thin liquid films have been done, for example, by Alekseenko *et al.*,[10] Alekseenko *et al.*,[11] Trifonov,[12] and Chang.[13] Their approximations are valid for larger Reynolds numbers than those allowed for the Benney equation.

The instability of thin liquid films has been investigated widely for flow down flat walls or flat cylinders. However, it is important too to investigate the instability of the fluid layer on walls with deformations. Mainly when the layer is very thin, the small roughness of the wall may play an important role in the development of the instability. The free surface response to large wall deformations has been investigated experimentally by Zhao and Cerro,[14] Shetty and Cerro,[15] Vlachogiannis and Bontozoglou,[16] and Decré and Baret.[17]

Some authors have proposed mathematical models with wall deformation, and their respective linear instabilities have been investigated by Bontozoglou and Papapolymerou,[18] Wierschem and Aksel,[19] and Davis and Troian.[20] Wierschem *et al.*[21] compares the theory developed by different authors with experiment. In the case of small Reynolds number flow, Scholle *et al.*[22] present a method of solution by means of holomorphic functions. Numerical analysis of the equations has been done by Pozrikidis[23] for slow flow using the boundary-integral method, and by Malamataris and Bontozoglou,[24] Khayat and Welke,[25] and Ovcharova[26] by means of full numerical analysis of the Navier-Stokes equations. Negny *et al.*[27,28] made numerical analysis and experiments on solid wavy vertical columns.

Other theoretical approaches to obtain nonlinear equations for the evolution of thin films that flow on wall deformations are the integral method or the Karman-Polhausen method applied by Trifonov[29,30] and by Valluri *et al.*[31] and the lubrication approximation applied by Kalliadasis *et al.*[32] and Bielarz and Kalliadasis.[33] Some asymptotic approximations done directly from the Navier-Stokes equations and boundary conditions have been performed by Tougou[34] and Wang[35,36] for a Newtonian fluid, and by Usha and Uma[37] for a viscoelastic fluid. Other approximations have been used by Alleborn and Rasziller.[38] They also give solutions to their linear equation.

In this paper, the nonlinear instability of a fluid layer flowing down a smoothly deformed wall is investigated. The

smooth wall approximation is assumed because the approach here will be to follow the same approximations done for the free surface deformation in the derivation of the Benney equation.[6,39–42] In this way, the wall deformation will come into play in the same way as the free surface, except that it is time-independent. The result will be a nonlinear evolution equation of the Benney type including the effects of wall deformation. To the best of my knowledge, this approach is new and has not been pursued before. Moreover, a surface time-dependent perturbation will be included in the equation in order to control the evolution of the frequency of perturbations that propagate on the free surface already deformed by the wall effects. In this way, a perturbed Benney equation with wall deformation effects will be calculated.

The structure of the paper is as follows. In the next section, the perturbed Benney equation including effects of the wall deformation is calculated. In Sec. III, numerical solutions of the equation are presented that include the evolution of surface time periodic perturbations. Sections IV and V are the discussion and conclusions, respectively.

II. THE PERTURBED BENNEY EQUATION WITH WALL DEFORMATION EFFECTS

In this section, the perturbed Benney equation including effects of the deformation of the solid boundary is calculated using the long-wave approximation. In this approximation, $\varepsilon=2\pi h_0/\lambda \ll 1$ is the small parameter. Here, h_0 is the thickness of the layer and λ is the effective wavelength, supposed very long. This means that the slope of the resulting free surface deformations should be small. The same scaling assumption is made also with respect to the wall deformations that should have a very small slope ε as that of the free surface. The variables have been made nondimensional by means of h_0 for distance perpendicular to the wall, $\lambda/2\pi$ for distance in the horizontal direction, $h_0^3/(\nu\lambda/2\pi)$ for time, ν/h_0 for velocity, and $\rho\nu^2/h_0^2$ for pressure. Here, ν is the kinematic viscosity and ρ is the density. If the original variables are capital letters, they are replaced by the nondimensional variables as $Z=h_0\bar{z}$, $(X,Y)=(\lambda/2\pi)(\bar{X},\bar{Y})$, $T=[h_0^3/(\nu\lambda/2\pi)]\bar{T}$, $U=(\nu/h_0)u$, and $P=(\rho\nu^2/h_0^2)p$, respectively. The scale discrepancy among the variables is better shown using the small parameter ε. Then the variables are scaled as $x=\varepsilon\bar{x}$, $y=\varepsilon\bar{y}$, $z=\bar{z}$, and $t=\varepsilon\bar{t}$, where the overbar over the lower-case letters means that only h_0 was used to make them nondimensional.

The coordinate system is set considering flow going down a flat wall. Thus, the flow is in the x direction perpendicular to the z direction, which crosses the film thickness pointing outwards from the fluid film. The wall is located at $z=0$. Perpendicular to these two directions in a right-handed system is the y direction. With this coordinate system, it is possible to have a reference to set the wall deformations and the surface deformations appearing as a response to the wall profile.

Then, the nondimensional Navier-Stokes and continuity equations are scaled as

$$\varepsilon u_t+\varepsilon u u_x+\varepsilon v u_y+w u_z=-\varepsilon p_x+\varepsilon^2 u_{xx}+\varepsilon^2 u_{yy}+u_{zz}+\mathrm{Re}\sin\beta, \tag{1}$$

$$\varepsilon v_t+\varepsilon u v_x+\varepsilon v v_y+w v_z=-\varepsilon p_y+\varepsilon^2 v_{xx}+\varepsilon^2 v_{yy}+v_{zz}, \tag{2}$$

$$\varepsilon w_t+\varepsilon u w_x+\varepsilon v w_y+w w_z=-p_z+\varepsilon^2 w_{xx}+\varepsilon^2 w_{yy}+w_{zz}-\mathrm{Re}\cos\beta, \tag{3}$$

$$w_z=-\varepsilon u_x-\varepsilon v_y. \tag{4}$$

Subindexes x, y, z, and t mean partial derivatives. The boundary conditions are evaluated at the wall and at the free surface. At the wall, the nonslip condition is

$$u=v=w=0 \quad \text{at } z=Q(x,y), \tag{5}$$

where $Q(x,y)$ is the smooth wall deformation. When $Q(x,y)=0$, the wall is flat. The normal stress boundary condition is

$$\begin{aligned}-p+\frac{1}{N^2}&[\varepsilon^3(u_x f_x^2+v_y f_y^2)+\varepsilon^3(u_y+v_x)f_x f_y\\&-\varepsilon(v_z+\varepsilon w_y)f_y-\varepsilon(u_z+\varepsilon w_x)f_x+w_z]\\&=P_p(x,y,t)-\frac{3}{N^3}\bar{S}[(1+\varepsilon^2 f_y^2)f_{xx}+(1+\varepsilon^2 f_x^2)f_{yy}\\&-2\varepsilon^2 f_x f_y f_{xy}] \quad \text{at } z=Q(x,y)+h(x,y,t),\end{aligned} \tag{6}$$

where $f(x,y,t)=Q(x,y)+h(x,y,t)$ and $N=\sqrt{1+\varepsilon^2 f_x^2+\varepsilon^2 f_y^2}$. Here $h(x,y,t)$ is the location of the free surface relative to the local wall deformation. Its magnitude varies around the nondimensional thickness 1. Even when there are no time-periodic perturbations [see Eq. (10)], $h(x,y,t)$ is a response of the fluid layer due to surface tension and shear stresses appearing when $Q(x,y)\neq 0$. The shear stresses are

$$\begin{aligned}\varepsilon(w_z-\varepsilon u_x)f_x-\tfrac{1}{2}\varepsilon^2(u_y+v_x)f_y+\tfrac{1}{2}(u_z+\varepsilon w_x)(1-\varepsilon^2 f_x^2)\\-\tfrac{1}{2}\varepsilon^2(\varepsilon w_y+v_z)f_x f_y=0 \quad \text{at } z=Q(x,y)+h(x,y,t)\end{aligned} \tag{7}$$

and

$$\begin{aligned}\varepsilon(w_z-\varepsilon u_y)f_y-\tfrac{1}{2}\varepsilon^2(u_y+v_x)f_x+\tfrac{1}{2}(v_z+\varepsilon w_y)(1-\varepsilon^2 f_y^2)\\-\tfrac{1}{2}\varepsilon^2(\varepsilon w_x+u_z)f_x f_y=0 \quad \text{at } z=Q(x,y)+h(x,y,t).\end{aligned} \tag{8}$$

The kinematic boundary condition is

$$w=\varepsilon h_t+\varepsilon u f_x+\varepsilon v f_y \quad \text{at } z=Q(x,y)+h(x,y,t). \tag{9}$$

A pressure of the form

$$P_p(x,y,t)=A\left|\sin\frac{\omega}{2}t\right|\exp[-a(x^2+y^2)], \tag{10}$$

with ω the frequency of oscillation, will be used later representing a turbulent air jet striking periodically on the free surface around the origin. For applications of a nonoscillating turbulent air jet, see Buchlin *et al.*[43] The constants of the pressure p_p in Eq. (10) will be taken as $A=0.0001$ and

$a=0.01$. The frequency ω is divided by 2 because a jet has no suction and it will have an effect only when it strikes again on the surface.

In the above equations, (u,v,w) are the velocity components in the (x,y,z) directions, respectively. The pressure is p, $h(x,y,t)$ is the local film thickness, and β is the angle of inclination. The Reynolds number is $\mathrm{Re}=gh_0^3/\nu^2$ and $S=\varepsilon^2\Sigma$, where $\Sigma=\sigma h_0/(3\rho\nu^2)$ is the nondimensional surface tension number where σ is the surface tension. The velocity scale used was ν/h_0 because this selection allows the $\sin(\beta)$ to be outside the Reynolds number. In this way, the Reynolds number is related with the volumetric flow rate by unit span q as $\mathrm{Re}=3q/\nu\sin(\beta)$.. Besides, note that Σ, apart from h_0, only includes fluid properties and it does not include gravity acceleration as the Weber number. Note that, in the present scaling, it is supposed that surface tension is very strong. Besides, in the small wavenumber approximation, the Reynolds number may have a magnitude above, but near, order 1.

The variables are expanded as

$$u=u_0+\varepsilon u_1+\cdots \quad v=v_0+\varepsilon v_1+\cdots,$$
$$w=\varepsilon(w_0+\varepsilon w_1+\cdots) \quad p=p_0+\varepsilon p_1+\cdots. \tag{11}$$

These are introduced into the equations of motion, continuity, and boundary conditions. The results to zeroth order are

$$p_0=-(z-Q-h)\mathrm{Re}\cos\beta-3S\nabla^2(Q+h)+P_p(x,y,t), \tag{12}$$

$$u_0=-\tfrac{1}{2}\mathrm{Re}\sin\beta(z-Q)(z-Q-2h), \tag{13}$$

$$w_0=-\tfrac{1}{2}\mathrm{Re}\sin\beta(z-Q)[(z-Q)(Q+h)_x-2\mathrm{hQ}_x], \tag{14}$$

$$h_t=-\mathrm{Re}\sin\beta h^2\frac{\partial h}{\partial x} \quad \text{at } z=Q(x,y)+h(x,y,t). \tag{15}$$

Here, at this order, $v_0=0$. It is understood that h is a function of (x,y,t), Q of (x,y), and p_0, u_0, and w_0 of (x,y,z,t).

The results to first order are

$$u_1=\tfrac{1}{24}(Q-z)[(\mathrm{Re}\sin\beta)^2u_{1a}h_x+u_{1b}\mathrm{Re}\sin\beta h_t+u_{1c}], \tag{16}$$

$$u_{1a}=hQ^3-3hQ^2z+3hQz^2-hz^3+4h^4,$$
$$u_{1b}=8Qz-4Q^2+12h^2-4z^4,$$
$$u_{1c}=-12\frac{\partial p_0}{\partial x}(z-Q-2h),$$
$$v_1=\frac{1}{2}\frac{\partial p_0}{\partial y}(Q-z)(Q+2h-z), \tag{17}$$

$$w_1=\tfrac{1}{120}(Q-z)\{(\mathrm{Re}\sin\beta)^2[(h_x)^2w_{1a}+h_xw_{1b}+h_{xx}w_{1c}]$$
$$+\mathrm{Re}\sin\beta(h_th_xw_{1d}+h_tw_{1e}+h_{xt}w_{1f})+h_xw_{1g}+w_{1h}\}, \tag{18}$$

$$w_{1a}=(Q-z)[(Q-z)^3+40h^3],$$
$$w_{1b}=5Q_xh[(Q-z)^3+4h^3],$$
$$w_{1c}=h(Q-z)[(Q-z)^3+10h^3], \quad w_{1d}=60h(Q-z),$$
$$w_{1e}=-20Q_x[(Q-z)^2-3h^2],$$
$$w_{1f}=-5(Q-z)[(Q-z)^2-6h^2],$$
$$w_{1g}=60p_{0x}(Q-z),$$
$$w_{1h}=60(Q-z+2h)(Q_xp_{0x}+Q_yp_{0y})$$
$$+20(Q-z)[3h_yp_{0y}+(Q-z+3h)(p_{0xx}+p_{0yy})].$$

These results are substituted in the first-order term of the kinematic boundary condition. That term will include h_t. This derivative is substituted by its value obtained at zeroth order, that is, by Eq. (15), along with the solution of p_0 given in Eq. (12). The final result, the evolution equation of the Benney type for the free surface deformation of a thin film flowing down an inclined wall with smooth deformations, is

$$h_t+\mathrm{Re}\sin\beta h^2h_x+\varepsilon\Big\{(\mathrm{Re}\sin\beta)^2\Big(\tfrac{2}{15}h^6h_x\Big)_x$$
$$+\tfrac{1}{3}\nabla\cdot\{h^3[-\mathrm{Re}\cos\beta\nabla(Q+h)$$
$$+3S\nabla^2\nabla(Q+h)-\nabla P_p]\}\Big\}=0. \tag{19}$$

It is clear that when the wall is flat, then $Q=0$ and the equation reduces to a perturbed Benney equation.[41] Moreover, if also $P_p=0$, the equation reduces to that of Benney.[6,8,39,40] This Eq. (19) will be solved numerically in the next section for a particular wall profile.

Let us assume that $P_p=Q=0$ and $h=1+H(x,t)$ in Eq. (19). After substitution, Eq. (19) is linearized with respect to $H(x,t)$. In the resulting equation, the variables are changed back into the nonscaled nondimensional variables. Now, let us suppose that $H(x,t)=A_1\exp i[kx-(i\Gamma+\omega)t]$ and A_1 is a small constant amplitude. Here, k is the wavenumber, Γ is the growth rate, and ω is the frequency. In this way, the real part of the equation gives the growth rate and the imaginary part gives the phase velocity, that is, $c=\omega/k=\mathrm{Re}\sin\beta$, which directly depends on the Reynolds number. The growth rate is

$$\Gamma=k^2\left(\frac{2\mathrm{Re}^2\sin^2\beta}{15}-\frac{1}{3}\mathrm{Re}\cos\beta-k^2\Sigma\right). \tag{20}$$

The neutral curves are obtained when $\Gamma=0$. Thus the critical wavenumber depends on Re as

$$k_c=\sqrt{\frac{1}{\Sigma}\left(\frac{2}{15}\mathrm{Re}^2\sin^2\beta-\frac{1}{3}\mathrm{Re}\cos\beta\right)}. \tag{21}$$

It can be shown that the wavenumber of the maximum growth rate is $k_m=1/\sqrt{2}k_c$. Gjevik[7] calculated the curve of subcriticality below which it was supposed that the surface waves could not saturate. Gjevik (see also Ref. 42) has shown that $k_s=1/2k_c$. These results are reviewed as follows:

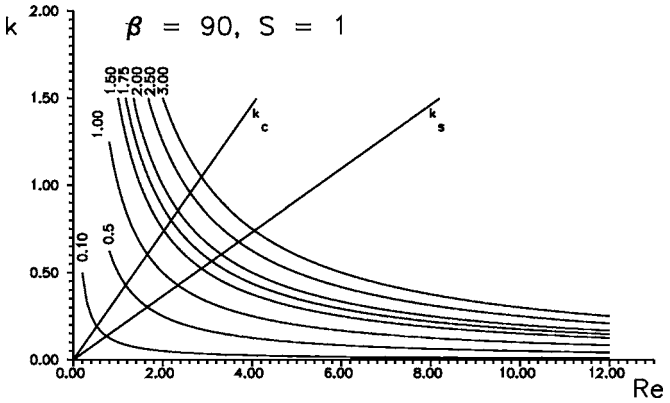

FIG. 1. Graphs of k vs Re for the case in which the wall is vertical. It shows the curves of criticality (below which instability occurs) and subcriticality, which are straight lines when $\beta=90°$. Between the curves k_c and k_s, the bifurcation is supercritical, and below k_s the bifurcation is subcritical. The numbers in the curves show the frequency of oscillation of the external perturbation applied at the free surface. The curves are calculated using $k=\omega/\mathrm{Re}\sin\beta$.

$$k_c^2 = 2k_m^2 = 4k_s^2. \tag{22}$$

It has been shown numerically[39,41] that, even below the curve of subcriticality, the waves described by the Benney equation are able to saturate. The curves described by Eq. (22) are plotted in Fig. 1 in the case of $\beta=90°$. The curves shown in Fig. 1 will be useful to understand the situation of the numerical results presented in the next section.

III. NUMERICAL ANALYSIS OF EQ. (19)

Here the numerical analysis of Eq. (19) is presented. The perturbations due to wall deformation and due to a time-periodic perturbation will be investigated in space and time. Here, variations in the y direction are neglected. To that goal, Eq. (19) will be analyzed using finite differences of first order in time and centered finite differences of second order in space. Calculations were made keeping $\mathrm{Re}\,\Delta t/(\Delta x)^2 < 0.01$. The wall will remain vertical ($\beta=90°$) and its profile will be that of sinusoidal deformations. It will be supposed that the wall deformation is zero at $x=0$, but numerical calculations will start from $x=-100$ until $\mathrm{Re}\,\Delta t+100$ ($\mathrm{Re}\sin\beta$ is the phase velocity).

The wall sinusoidal wavelength is determined as in $Q(x)=B\sin[x\omega/L\,\mathrm{Re}\sin\beta]$. It is clear that the wavelength of the wall deformation is taken as a multiple (L times, with L a real number) of the wavelength λ produced by the time-dependent surface perturbation $\mathrm{Re}\sin\beta/\omega=\lambda/2\pi=1/k$. B is the amplitude that will be fixed as 0.1. It was very useful numerically to suppose the wall wavelength in this fashion, as will be seen presently. The free surface response deformation presents spatial resonance (increase in amplitude) when the wavelength of the wall is reduced. Surely, this also occurs in the absence of surface time-periodic perturbations. In fact, if Eq. (19) is linearized with $h(x,y,t)=1+H(x,y,t)$ [$H(x,y,t)$ very small] using the assumption of a wavy wall in the form of a sine function and changing back to the original nonscaled nondimensional variables, a linear Benney equation is found with a sine forcing term on the right-hand side as follows:

$$H_t + \mathrm{Re}\sin\beta H_x + \frac{2}{15}(\mathrm{Re}\sin\beta)^2 H_{xx} + \frac{1}{3}(-\mathrm{Re}\cos\beta H_{xx} + 3SH_{xxxx}) = -\frac{1}{3}\left(\frac{\omega}{L\mathrm{Re}\sin\beta}\right)^2\left\{\left[\mathrm{Re}\cos\beta + 3S\left(\frac{\omega}{L\mathrm{Re}\sin\beta}\right)^2\right]\right\} \times B\sin\left[\frac{x\omega}{L\mathrm{Re}\sin\beta}\right]. \tag{23}$$

This resonance effect is felt by the nonlinear equation where the "forcing term" appears multiplied by powers of h and its derivatives. Therefore, it contributes to modify nonlinearly the surface response h. This resonant response appeared for all Reynolds numbers investigated inside the area between the curves of criticality and subcriticality and also below the curve of subcriticality. However, in this paper, only results with Reynolds numbers and wavenumbers below subcriticality are presented.

The figures that will be presented containing numerical results show two graphs each. The lower graphs of the figure are the results of calculations done during a given time interval. For the sake of visualization, the upper graphs of the figure are an amplification in some space interval of the lower graphs. The graphs without time-periodic perturbations show two curves. The one below corresponds to the wall profile. Note that the wall profile is not plotted with its center at -1 units of the ordinates axis. It is plotted as shown only for the sake of comparison and presentation. The curves above are the free surface response to the wall profile. The figures with time-periodic perturbations include an extra curve that corresponds to the waves on the free surface of a thin film flowing down a flat surface. This allows us to compare the surface wave with that propagating on a surface responding to the wall profile. Note that all the results presented here will correspond to time-dependent perturbations below subcriticality (see Fig. 1).

For the case of an imposed frequency $\omega=0.1$ and $\mathrm{Re}=1$, results are shown in Figs. 2 and 3. In those figures, the wavelength of the wall is three times ($L=3$) that of the surface time-periodic perturbation. It may be seen in Fig. 2 that the free surface response is slightly out of phase with respect to the wall. It is clear in Fig. 3 that the time-periodic perturbation is present in the entire time interval of the calculation, which is $t=2000$. It is also possible to compare the form of the perturbations appearing when the wall is wavy and flat.

The following numerical results are similar to those shown in Figs. 2 and 3, except that here $L=1.25$. These are shown in Figs. 4 and 5. The valleys in the curves are deeper than before. This has an important effect on the time-periodic perturbations, which disappear with distance as seen in the amplification shown in Fig. 5. This amplification is identical to that of Fig. 4. An explanation of this phenomenon is that

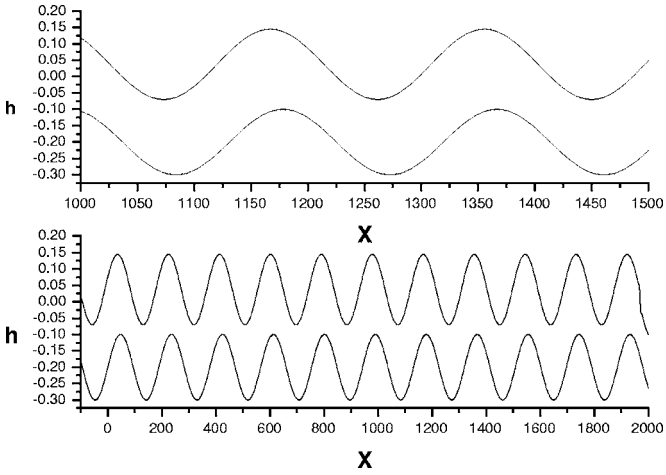

FIG. 2. No time-dependent perturbation corresponding to a wall wavelength three times that of the perturbation wavelength ($L=3$) with $\omega=0.1$ and Re=1. The time is $t=2000$. The lower graph corresponds to the full-time calculation. The upper graph is an expansion of a section of the lower one. The curves in each graph are the wall profile, shown below, and the free surface response, shown above. Notice that the center of the wall profile should be located at −1 with respect to the ordinates axis. The position was selected for the sake of presentation.

when the free surface response to the wall shows deeper valleys, the time-dependent perturbations spend more time in them, where the thickness of the layer corresponds locally not only to a lower Reynolds number but also to a stabilizing one, and consequently the perturbation starts to stabilize. The perturbation may recover at the top of the free surface response, where locally the Reynolds number is higher, but it has not enough time to grow stronger again. The deeper the valley is, the stronger the stabilizing effect. After traveling through a few valleys, the perturbations are not able to grow again and disappear.

Another example is presented in the case of $\omega=2$ and Re=4. In this case, the time interval of the full numerical

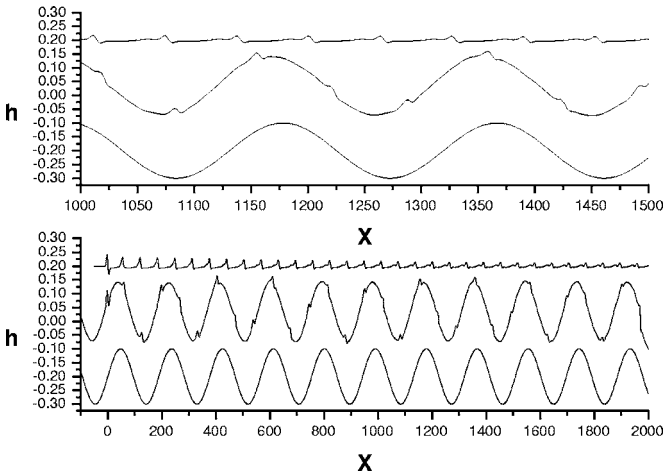

FIG. 3. Time-dependent perturbation with $\omega=0.1$, Re=1, and $L=3$. All the same as in Fig. 2 except that here, for the sake of comparison, a third extra curve is plotted above corresponding to the surface wave of a film flowing down a flat wall. Notice that the waves excited by time-periodic perturbations propagate superposed to the wave response of the free surface due to the wall waviness. The perturbations are seen in the entire time range.

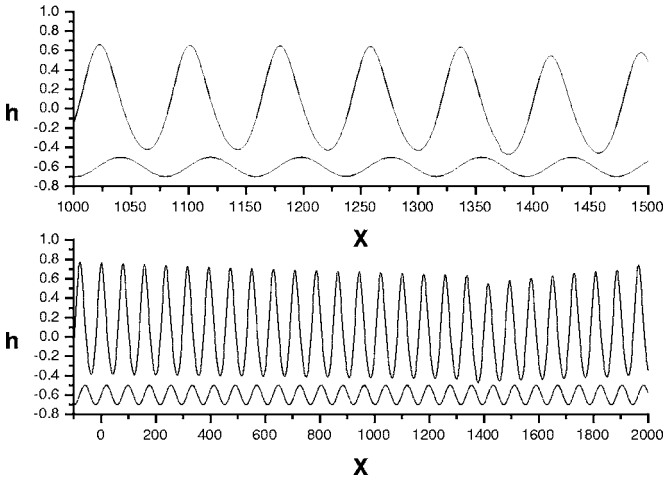

FIG. 4. The same as in Figs. 2 and 3 but here $L=1.25$. The valleys are deeper.

calculation is $t=1200$. The wave has a drastic difference with respect to the one shown before. The magnitude of the Reynolds number may give the impression that the time-periodic perturbations might not be able to disappear. It will be shown that this is not the case. Figures 6 and 7 present numerical results for the case $L=7$. Results in the absence of time-periodic perturbations are shown in Fig. 6. The perturbation wavelength is very small, but the wall has $L=7$ times that value. In Fig. 7, the time-periodic perturbations are included. They seem to be solitary waves under modulation. They also appear far away from their onset on the free surface response due to the wavy wall. However, by comparison, it is clear that their amplitude with respect to the free surface response is shorter than in a flat wall. Despite this effect, the perturbation solitary waves seem to be very strong and do not decrease notably with distance. Next, the wavelength of the wall profile is decreased to three times that of the time-periodic perturbation. As seen in Fig. 8, the surface response is very strong and the valleys become very deep and different from a sinusoidal wave due to the influence of the wall pro-

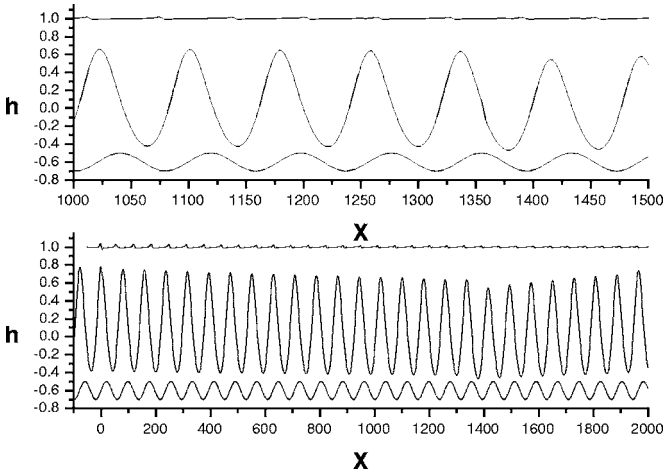

FIG. 5. The same as in Figs. 2 and 3 except that here $L=1.25$. The valleys are deeper. Note, in the amplification above the figure, that the time-periodic perturbations already disappeared in that interval.

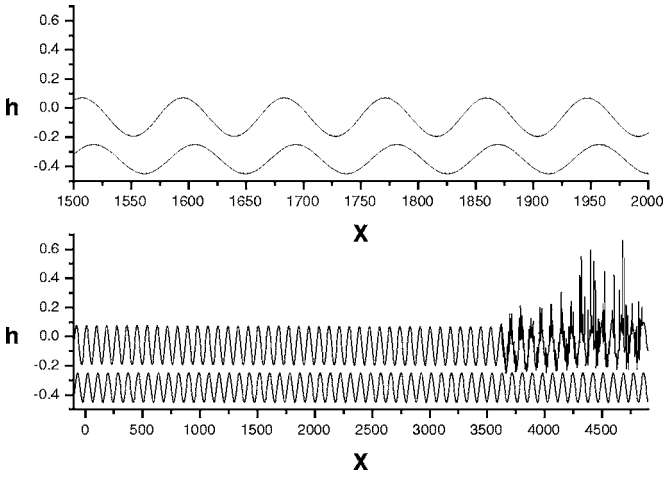

FIG. 6. No time-periodic perturbations. Here $\omega=2$ and Re$=4$ and $L=7$. The time of the full numerical calculation is $t=1200$. The perturbation wavelength is very small. The wall profile has seven times that wavelength. The waves appearing at the right are transients.

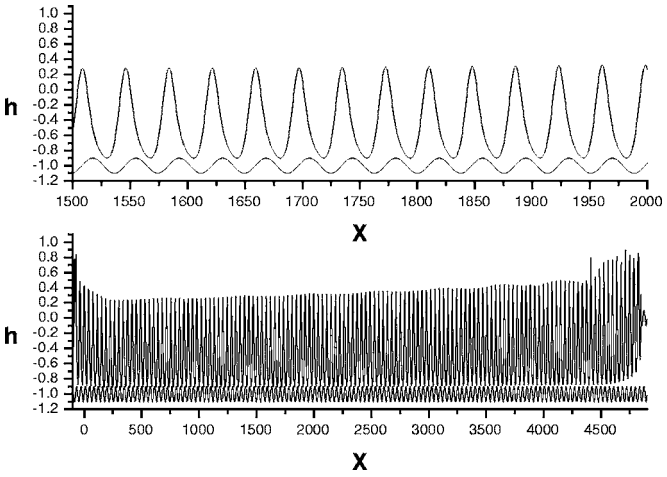

FIG. 8. No time-periodic perturbations. Here $\omega=2$ and Re$=4$ and $L=3$. The perturbation wavelength is very small and the wall wavelength is only three times its value. The valleys are deeper and they are modified by the wall profile in such a way that they differ clearly from the sinusoidal wave.

file. This has important consequences on the time-periodic perturbations, as shown in Fig. 9. Here, the perturbations are already absent at the distance shown in the amplified space interval. Therefore, even the solitary waves can be eliminated by a free surface response with deep valleys. When time-dependent perturbations are present, there always exist transient large perturbations that run in front of the surface waves. This was seen when the wall was both flat and wavy. As explained above, the free surface deformation time evolution was calculated numerically for both cases in the presence and absence of time-dependent perturbations. The calculations began from $t=0$ to a convenient final time. When the Reynolds number is very large, the spatial perturbations due to the wall deformation began to produce transient free surface deformations that were carried away in time by the incoming flow, as shown in Fig. 6. These waves have very large saturated amplitude but produce no influence on the surface deformation under study moving behind them. These waves may be thought to be generated as if the wall was not inclined at the onset and then, instantly, it was inclined to generate the flow under research.

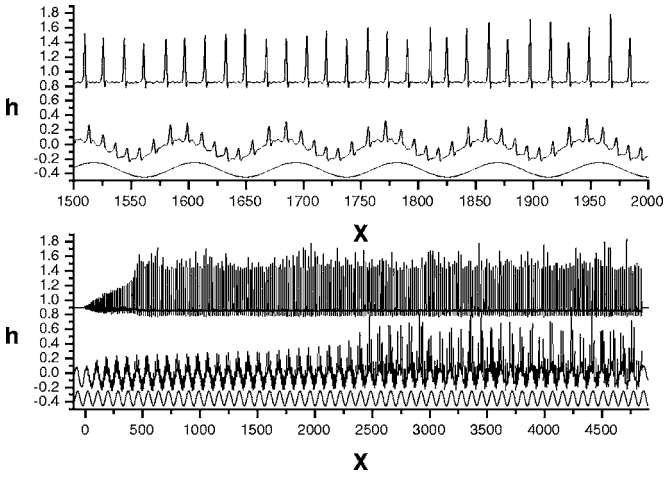

FIG. 7. Time-periodic perturbations. The same as in Fig. 6. Note that, in the case of a flat wall, the surface waves could be modulated solitary waves. In the case of a wavy wall, the solitary waves are modified: their height with respect to the free surface response to the wall is shorter than in the case of a flat wall. However, it seems that they are not decreasing with distance.

IV. DISCUSSION

All the results presented here show the possibility of applying special wall profiles to eliminate time-periodic perturbations. Note that the numerical results for the perturbations shown in this paper correspond to a wavenumber and Reynolds number below the curve of subcriticality. They represent very unstable but saturated nonlinear waves. More results have been obtained for perturbations above the curve of subcriticality, and they also show success in eliminating the perturbations at particular values of L. Besides, based on the present results, it may also be possible to eliminate random perturbations, which will disappear after traveling through a few deep enough free surface response valleys. However, what might be the optimal depth of those valleys?

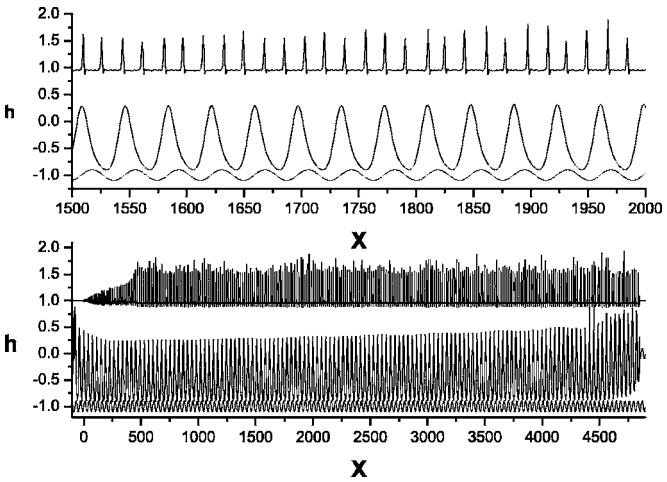

FIG. 9. Time-periodic perturbations. The same as in Fig. 8. Here, the perturbations disappear with distance.

If the valleys are very deep, the problem of dewetting will prevent the existence of a uniform wavy fluid layer. Then, detailed research using different values of L is needed in order to find out a valley thickness that avoids dewetting and that at the same time could cause the free surface time-periodic perturbations to disappear.

V. CONCLUSIONS

In this paper, an evolution equation has been calculated that describes the three-dimensional free surface response to a smoothly deformed wall. This equation also describes the evolution of free surface time-periodic perturbations propagating on the free surface response to the wall. It has been shown, for the particular case of a two-dimensional sinusoidal wavy wall, that the wavelength of the wall has a strong influence on the free surface response. It was found, from the linear point of view, that the waviness of the wall works as a forcing term in the linear evolution equation and that it produces a "spatial" resonance effect when the wall wavelength is reduced, generating an increase in amplitude of the free surface response. Note that the free surface response and the time-periodic perturbations superpose nonlinearly. The time-periodic perturbations show different amplitudes when propagating on the free surface response from those in the case of a flat wall (see, for example, Fig. 7). It was shown that the deeper the valley, the stronger the stabilizing effect is on the time-periodic perturbations. Finally, it is concluded that a passive process like this could be of importance in coating applications because if a finite but large enough number of waves are included in the wall upstream the area we are willing to coat, it might be possible to filter persistent ambient time-periodic perturbations.

ACKNOWLEDGMENTS

The author would like to acknowledge technical support from Raul Reyes, Cesar Díaz, Caín Gonzáles, and Victor Gómez.

[1] S. J. Weinstein and K. J. Ruschak, "Coating flows," Annu. Rev. Fluid Mech. **36**, 29 (2004).
[2] D. Quéré, "Fluid coating on a fiber," Annu. Rev. Fluid Mech. **31**, 347 (1999).
[3] C.-S. Yih, "Stability of liquid flow down an inclined plane," Phys. Fluids **6**, 321 (1963).
[4] S. P. Lin, "Instability of a liquid film flowing down an inclined plane," Phys. Fluids **10**, 308 (1967).
[5] J. M. Floryan, S. H. Davis, and R. E. Kelly, "Instabilities of a liquid film flowing down a slightly inclined plane," Phys. Fluids **30**, 983 (1987).
[6] D. J. Benney, "Long waves on liquid films," J. Math. Phys. (Cambridge, Mass.) **45**, 150 (1966).
[7] B. Gjevik, "Occurrence of finite-amplitude surface waves of falling liquid films," Phys. Fluids **13**, 1918 (1970).
[8] G. J. Roskes, "Three-dimensional long waves on a liquid film," Phys. Fluids **13**, 1440 (1970).
[9] G. I. Sivashinsky and D. M. Michelson, "On irregular wavy flow of a liquid film down a vertical plane," Prog. Theor. Phys. **63**, 2112 (1980).
[10] S. V. Alekseenko, V. Y. Nakoryakov, and B. G. Pokusaev, "Wave formation on a vertical falling liquid film," AIChE J. **31**, 1446 (1985).
[11] S. V. Alekseenko, V. Y. Nakoryakov, and B. G. Pokusaev, *Wave Flow of Liquid Films* (Begell House, New York, 1994).
[12] Y. Y. Trifonov, "Transition of two-dimensional wave flows to three-dimensional wave flows for vertically falling liquid film," Russ. J. Eng. Thermophys. **1**, 153 (1991).
[13] H.-C. Chang, "Wave evolution on a falling film," Annu. Rev. Fluid Mech. **26**, 103 (1994).
[14] L. Zhao and R. L. Cerro, "Experimental characterization of viscous film flows over complex surfaces," Int. J. Multiphase Flow **18**, 495 (1992).
[15] S. Shetty and R. L. Cerro, "Flow of a thin film over a periodic surface," Int. J. Multiphase Flow **19**, 1013 (1993).
[16] M. Vlachogiannis and V. Bontozoglou, "Experiments on laminar film flow along a periodic wall," J. Fluid Mech. **457**, 133 (2002).
[17] M. M. Decré and J. C. Baret, "Gravity-driven flows of viscous liquids over two-dimensional topographies," J. Fluid Mech. **487**, 147 (2003).
[18] V. Bontozoglou and G. Papapolymerou, "Laminar film flow down a wavy incline," Int. J. Multiphase Flow **23**, 69 (1997).
[19] A. Wierschem and N. Aksel, "Instability of a liquid film flowing down an inclined wavy plane," Physica D **186**, 221 (2003).
[20] J. M. Davis and S. M. Troian, "Generalized linear stability of noninertial coating flows over topographical features," Phys. Fluids **17**, 072103 (2005).
[21] A. Wierschem, M. Scholle, and N. Aksel, "Comparison of different theoretical approaches to experiments on film flow down an inclined wavy channel," Exp. Fluids **33**, 429 (2002).
[22] M. Scholle, A. Wierschem, and N. Aksel, "Creeping films with vortices over strongly undulated bottoms," Acta Mech. **168**, 167 (2004).
[23] C. Pozrikidis, "The flow of a liquid film along a periodic wall," J. Fluid Mech. **188**, 275 (1988).
[24] N. A. Malamataris and V. Bontozoglou, "Computer aided analysis of viscous film flow along an inclined wavy wall," J. Comput. Phys. **154**, 372 (1999).
[25] R. E. Khayat and S. R. Welke, "Influence of inertia, gravity, and substrate topography on the two-dimensional transient coating flow of a thin Newtonian fluid film," Phys. Fluids **13**, 355 (2001).
[26] A. S. Ovcharova, "Controlling the free-surface profile of film flow over complex topography," J. Appl. Mech. Tech. Phys. **45**, 523 (2004).
[27] S. Negny, M. Meyer, and M. Prevost, "Study of a laminar falling film flowing over a wavy wall column. Part I: Numerical investigation of the flow pattern and the coupled heat and mass transfer," Int. J. Heat Mass Transfer **44**, 2137 (2001).
[28] S. Negny, M. Meyer, and M. Prevost, "Study of a laminar falling film flowing over a wavy wall column. Part II: Experimental validation of hydrodynamic model," Int. J. Heat Mass Transfer **44**, 2147 (2001).
[29] Y. Y. Trifonov, "Viscous liquid film flows over periodic surface," Int. J. Multiphase Flow **24**, 1139 (1998).
[30] Y. Y. Trifonov, "Viscous film flow down corrugated surfaces," J. Appl. Mech. Tech. Phys. **45**, 389 (2004).
[31] P. Valluri, O. K. Matar, G. F. Hewitt, and M. A. Mendes, "Thin film flow over structured packings at moderate Reynolds numbers," Chem. Eng. Sci. **60**, 1965 (2005).
[32] S. Kalliadasis, C. Bielarz, and G. M. Homsy, "Steady free-surface thin film flows over topography," Phys. Fluids **12**, 1889 (2000).
[33] C. Bielarz and S. Kalliadasis, "Time-dependent free-surface thin film flows over topography," Phys. Fluids **15**, 2512 (2003).
[34] H. Tougou, "Long waves on a film flow of a viscous fluid down an inclined uneven wall," J. Phys. Soc. Jpn. **44**, 1014 (1978).
[35] C.-Y. Wang, "Liquid film flowing slowly down a wavy incline," AIChE J. **27**, 207 (1981).
[36] C.-Y. Wang, "Thin film flowing down a curved surface," ZAMP **35**, 532 (1984).
[37] R. Usha and B. Uma, "Long waves on a viscoelastic film flow down a wavy incline," Int. J. Non-Linear Mech. **39**, 1589 (2004).
[38] N. Alleborn and H. Raszillier, "Local perturbation of thin film flow," Arch. Appl. Mech. **73**, 734 (2004).
[39] S. W. Joo, S. H. Davis, and S. G. Bankoff, "Long-wave instabilities of heated falling films: Two-dimensional theory of uniform layers," J. Fluid Mech. **230**, 117 (1991).
[40] S. W. Joo and S. H. Davis, "Instabilities of three-dimensional viscous falling films," J. Fluid Mech. **242**, 529 (1992).
[41] L. A. Dávalos-Orozco, S. H. Davis, and S. G. Bankoff, "Nonlinear instability of a fluid layer flowing down a vertical wall under imposed time-periodic perturbations," Phys. Rev. E **55**, 374 (1997).
[42] L. A. Dávalos-Orozco and F. H. Busse, "Instability of a thin film flowing

on a rotating horizontal or inclined plane," Phys. Rev. E **65**, 026312 (2002).
[43] J.-M. Buchlin, M. Manna, M. Arnalsteen, M. L. Riethmuller, and M. Dubois, "Theoretical and experimental investigation of gas-jet wiping," in *Proceedings of the 1st European Coating Symposium on the Mechanics of Thin Film Coating*, Leeds University, UK, 1995, edited by P. H Gaskell, M. D. Savage, and J. L. Summers (World Scientific, Singapore, 1996), pp. 168–178.